Simultaneous Multitemperature Measurements of Thermal Diffusivity and Composition

Y. W. Kim

Abstract   It has been well established that thermal forcing of disordered multielement metallic alloys results in permanent modification of their thermal transport properties. The mechanism depends on the detail of heating and its duration, and entails rearrangement of the spatial distribution of constituent atoms within the material proper. It presents a serious complication in developing a body of properties data as a function of temperature because establishment of a thermal state for a specimen is often cast into question. A new general technique is presented for simultaneous multiple-temperature measurements of thermal diffusivity and local composition for a single specimen. The specimen is heated steeply into a state of temperature nonuniformity. The measurement is carried out by time-resolved spectroscopy of single-shot laser-produced plasma (LPP) plume emissions; analysis is made of the emissions as a function of position within the laser focal area. The procedure for analysis is presented together with the results for 80 mass% Ni-20 mass% Cr Nichrome specimens.

1 Introduction

The great majority of metallic alloys that are in use are disordered multielement alloys. They are exposed to a wide range of temperature during their lifetime of utilization. Examples of high-temperature applications range from energy production processes, such as in fission and fusion reactors and chemical process reactors to pyrometallurgical processors. Their thermophysical properties have been found to deviate from

Y. W. Kim (✉)
Lewis Laboratory #16, Department of Physics, Lehigh University, Bethlehem, PA 18015-3182, USA
e-mail: ywk0@lehigh.edu

the design specifications as the exposure time to elevated temperatures accumulates. We have investigated the thermophysical properties in the high-temperature regime for a number of disordered metallic alloy specimens by using the method of real-time spectroscopy of laser-produced plasma (LPP) plume emissions from a specimen surface. This method has the unique capability of providing both thermal-diffusivity and elemental-composition measurements simultaneously from each LPP plume [1]. Examination of a specimen after each different thermal forcing shows that changes in thermophysical properties are unambiguously linked to modifications of the near-surface elemental composition. Repetitive applications of the LPP analysis on the same surface spot of the specimen produce a near-surface composition profile as a function of depth into the bulk. Such profiles show distinct departures from the bulk composition, and thicken with increasing duration of thermal forcing and the temperature to which the specimen has been heated. It is found to be rarely reversible.

Several physical mechanisms are involved in this type of thermal cycling: heating, thermal expansion, structural phase transformation, atom diffusion, and cooling. At times, even melting and solidification come into play. To narrow the diversity of thermal forcing mechanisms, the usual procedure is to carry out transport property measurements at each freshly heated state for a specimen. However, this procedure is extremely time-consuming and labor-intensive. Besides, the final temperature of heating alone does not fully specify the effect imparted on the specimen.

In this paper, we describe a new procedure for carrying out measurements of thermophysical properties at several temperatures all at once by the method of LPP plume emission spectroscopy. When a long ribbon-shaped specimen is clamped at its two ends by heavy electrodes and heated electrically, the ribbon along its long axis exhibits a zone at each end that is steeply nonuniform in temperature. These zones are examined by the method of LPP plume spectroscopy. Position-resolved analysis of LPP plume emissions following a single laser-pulse excitation with a spatially extended footprint [2] can provide a set of measurements of both the thermal diffusivity and elemental composition at multiple temperatures within a microsecond.

The method for creating a nonuniform temperature zone and analyzing the structure of the LPP plume and the procedure for extraction of elemental composition and thermal diffusivity are described in the following sections. The results of thermophysical property measurements are also presented for a specimen of 80 mass% Ni-20 mass% Cr Nichrome alloy.

2 Experimental Setup for Analysis of Nonuniform Heated Specimens

The specimen preparation, heating, and LPP analysis are conducted within a vacuum chamber that has a full range of sensors and observation ports. The high power laser pulse is brought into the vessel through a focusing lens at the top of the vessel; the lens also serves as a vacuum window. The specimen is mounted within a cylindrical mechanical feed-through, which is inserted into the vacuum vessel through a vacuum coupling port. The feed-through can be moved into, and out of, the vessel by measured distances by means of a set of fixed thickness stops, and rotated about its own long axis.

The dimensions of the Nichrome ribbon specimen are 33 mm long, 4 mm wide, and 0.23 mm in thickness. The specimen is folded 1 mm from each end and pinched flat at both ends, and loaded onto the specimen holder by latching into the flat jaws of the respective electrode blocks. When fully assembled, the specimen holder maintains the specimen under constant tension at approximately 5 N throughout the heating and measurement period.

The specimen is heated by a 60 Hz ac current in the range of 20 A to 30 A in a steady-state mode, where the influence of an electric field on atom transport is minimal due to the alternating nature of the ac field [3]. The specimen temperature is measured by an alumel–chromel thermocouple junction during the heating; the wires are each 0.25 mm in diameter, and the junction is approximately circular in cross section and 0.6 mm in diameter. The junction is mounted on a vacuum flange below the specimen holder through a vacuum feed-through. The flange is organized as a motion feed-through so that the thermocouple can be translated linearly along the long axis of the specimen by means of a micrometer driven translation mechanism. In operation, the specimen is first heated, and the thermocouple tip is aligned and raised into contact with the specimen from below. The LPP analysis is made on the top-side surface of the specimen. We have noticed that the red glow of the specimen under heating dims very slightly when the thermocouple makes contact with the specimen. The tip of the junction is not mechanically rigid by necessity. We estimate that the combined measurement uncertainty is 0.5 mm in axial position and about 10 K below the local absolute temperature of the specimen.

When the heating current is turned on, the temperature of the specimen rises rapidly to a pseudo steady-state value within the first 15 s but slowly creeps upward in the next tens of minutes, heating up the specimen feed-through. The thermocouple is brought into contact with the specimen only when the temperature is measured once every 2 min to 5 min.

After the initial evaluation and calibrations runs, all LPP runs were made near the edge of the electrode clamp, where the temperature gradient is still large. The measurement has been made near one edge of the specimen ribbon, about 5 mm from the clamp, where both the temperature and its gradient are large; near the center of the ribbon, the temperature becomes uniform. In this region of a high-temperature gradient, the laser pulse is incident on an elliptical base area, from which the LPP plume emerges. The focal area is 2.3 mm wide and 1.3 mm long along the axis of the temperature gradient. The 1:1 image of the plume is formed on the entrance slit plane of the spectrograph; the long axis of the slit is aligned with the direction of the temperature gradient. A two-dimensional array detector positioned at the image plane of the spectrograph captures the individual LPP plume emission spectra emanating from 256 contiguous area elements on the specimen. The notion of simultaneous multiple-temperature measurement of thermophysical properties of the specimen is thus realized in this imaging spectroscopy implementation.

Twenty successive LPP spectra are taken from a fixed area of a fresh unheated Nichrome specimen for reference. They show that the topmost surface layer has an elemental composition that is slightly richer in chromium than in the bulk, but the rest of the succeeding LPP spectra shows a uniform composition profile in depth [1,4]. The final measurements were made at a fixed position, 5.2 mm from the electrode

clamp, at three different temperatures. The temperature span at this spot was shifted by changing the ac heating current. The temperature gradient was determined from three measured temperatures, one at the spot of LPP analysis and two others at a location 3.2 mm away on either side, each at different Ohmic heating current settings. The specimen was heated from a freshly cut specimen for a total of 17 min from the start of heating to the completion of the LPP measurements; the measurement proceeded for the specimen from the lowest to the highest temperature. The time between two successive LPP runs ranged from 2 min and 4 min.

3 LPP Analysis and Calibration

The intensity distribution of the laser pulse incident on the specimen surface is not uniform across the focal spot area. The thickness of laser-ablated matter, θ, scales with thermophysical properties according to the empirical scaling relation of the following form [5]:

$$\theta = C D_T^{\alpha} M^{\beta} H_{\text{f}}^{\gamma}, \tag{1}$$

where θ is the ablation thickness in cm and D_T is the thermal diffusivity in $\text{cm}^2 \cdot \text{s}^{-1}$. M is the molar mass for the specimen alloy, and H_{f} is the heat of formation in $\text{J} \cdot \text{g}^{-1}$. In vacuum, $\alpha = 0.91 \pm 0.01$, $\beta = -\alpha$, and $\gamma = -1$. C is the scaling constant at a fixed laser pulse energy, such that the product on the right-hand side of Eq. 1 gives rise to the thickness of the ablated matter in cm. The validity criterion is satisfied when the laser ablation is driven in pace with the propagation of the thermal diffusion front into the specimen; under such a condition, disparate constituent elements are ablated in proportion to the local elemental composition. The spectral intensities of the plume emissions become highly reproducible.

Now that we are pursuing simultaneous multitemperature determination of the thermal diffusivity and elemental composition, nonuniformity of the laser intensity profile must be calibrated across the focal spot along the temperature gradient axis because local mass loss by ablation is laser intensity dependent. We have chosen to use the fresh specimen at room temperature as the reference by carrying out the LPP analysis at identical laser power densities using the same optical, spectroscopic, and plasma plume timing setup [6]. We have thus chosen position-resolved LPP plume spectra from the 15th LPP excitation of the unheated fresh specimen as the reference. The measures of thermal diffusivity of the Nichrome specimen at elevated temperatures are expressed relative to the reference specimen at room temperature; extraction of the thermal diffusivity from the mass loss measurement is treated in the next section.

Figure 1 shows two sets of LPP plume emissions: one from a specimen that is heated nonuniformly to 1,033 K at the center of the laser focal spot and the second from the reference specimen at room temperature. Each set is composed of 256 spectra from an area patch of the specimen, 10 μm wide by 100 μm long. Altogether 256 such patches are aligned lengthwise contiguously along the entrance slit of the spectrograph; the temperature of each succeeding patch decreases. The emission spectrum from a given area patch is detected by a row of 1,024 detector pixels.
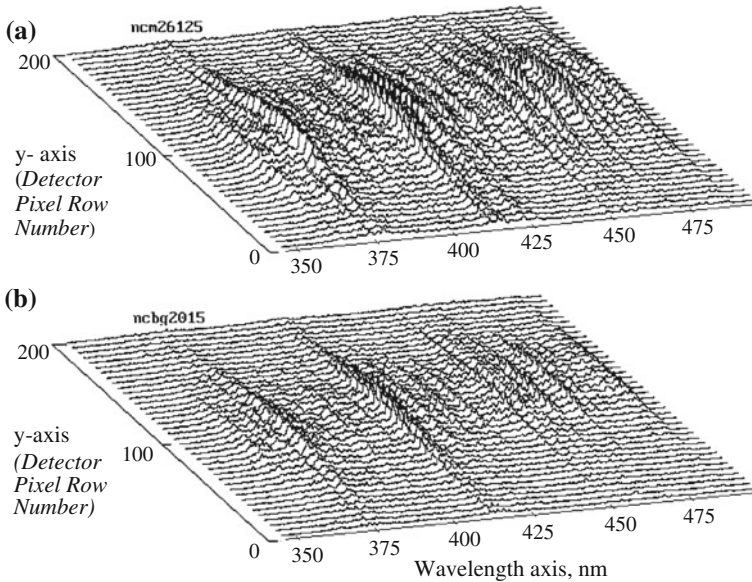
Fig. 1 LPP plume emission spectra from: (**a**) nonuniformly heated Nichrome specimen at about 1,033 K at the center of the laser focal area and (**b**) fresh Nichrome specimen as a reference at room temperature. The temperature decreases linearly with increasing *y*-axis position (pixel row address) along the specimen's long axis of symmetry. The emission intensity spectra from different plasma base area elements, each 10 μm wide by 100 μm long, are shown as a function of the base area address (detector pixel row address); the spectra are shown for every fifth area along the entrance slit of the spectrograph. The integration time is 600 ns

The mass loss due to LPP excitation is obtained from combined intensities of the representative emission lines from nickel and chromium. In equilibrium plasma, the line emission intensity at a given wavelength, as integrated by the detector, is determined by the number of atoms within the radiating plasma volume element multiplied by the atomic transition probability of the emission line. Transition probabilities vary widely according to the atomic structure, however, and must be rescaled in proportion to the elemental abundances of nickel and chromium within the radiating volume [7,8]. The rescaled intensities of nickel emission lines at 440.155 nm and 471.442 nm and of chromium lines at 425.435 nm, 427.48 nm, and 428.972 nm are combined into a hybrid measure of the mass of radiating atomic species that is undetermined within a constant. This undetermined constant is fixed by calibrating against the mass loss determined by weighing the reference specimen after 100 LPP exposures at room temperature; a digital microbalance (Mettler Toledo) of 0.1 μg resolution is used to determine the change in the specimen mass per LPP exposure at the same laser pulse intensity. The average mass loss from the fresh reference specimen due to LPP excitation is found to be (0.25 ± 0.02) μg per shot. This corresponds to an average depth of ablation of 12.1 nm per shot into the bulk of the reference specimen. Elemental composition of each LPP plume is measured from the LPP spectrum, and therefore both the total mass loss and ablation depth are obtained for each LPP excitation. The position-resolved

emission spectra are then analyzed using the same set of emission lines according to the mass loss calibration protocol described above.

4 Relative Thermal Diffusivity as a Function of Temperature

The scaling relation of Eq. 1 can be rewritten as follows:

$$D_T(T) = \left[\frac{\Delta m(T)}{C \rho(T)} H_f(T) \right]^{\frac{1}{\alpha}} M(T). \tag{2}$$

Here $\Delta m(T)$ denotes the mass loss. The thermal diffusivity of the heated test specimen, relative to the thermal diffusivity of the fresh specimen at room temperature, can then be expressed as a function of temperature as

$$\frac{D_T(T)}{D_T(T_{rm})} = \left[\frac{\Delta m(T)}{\Delta m(T_{rm})} \frac{\rho(T_{rm})}{\rho(T)} \frac{H_f(T)}{H_f(T_{rm})} \right]^{\frac{1}{\alpha}} \frac{M(T)}{M(T_{rm})}, \tag{3}$$

where T_{rm} denotes room temperature. In addition to the relative mass loss which we have at hand from the measurement, we must have the relative mass density, relative heat of formation, and relative molar mass in order to complete the conversion as a function of temperature.

The mass density of the specimen changes due to thermal expansion, and we write in the limit of small expansion,

$$\rho(T) = \rho(T_{rm}) \left[1 + \xi_T(T)(T - T_{rm}) \right]^{-3}. \tag{4}$$

We have measured the coefficient of linear thermal expansion of the Nichrome specimen over the range of temperature that has been explored in this study and found it to be reasonably well approximated by a constant value: $\xi_T \cong 1.5 \times 10^{-5} \, \mathrm{K}^{-1}$ (R. Cress, unpublished, 2008)[9].

The heat of formation must decrease with increasing temperature because thermal excitation raises the expectation value of the two-particle bound state energy and this reduces the energy cost for vaporization. In the absence of explicitly Nichrome data, we adopt a model successfully tested for water [10];

$$H_f(T) = H_m(T_m) + H_e(T) = H_m(T_m) + H_e(T_{rm}) \left(\frac{T_{cr} - T}{T_{cr} - T_{rm}} \right)^{0.375}, \tag{5}$$

where $H_m(T_m)$ is the latent heat of melting at the melting point temperature T_m. $H_e(T)$ and $H_e(T_{rm})$ are the latent heat of evaporation at temperature T and at room temperature T_{rm}, respectively. T_{cr} denotes the critical temperature: we choose the value for nickel, which is 9,460 K [11]. Finally, the molar mass changes with temperature due to the fact that the near-surface composition of the specimen changes at elevated temperatures, and the ablated matter by LPP excitation is from the local specimen's surface

Fig. 2 Relative thermal diffusivity is shown as a function of position along the long axis of specimen symmetry, as deduced from analysis of the spectral data shown in Fig. 1, together with (**a**) the specimen temperature, (**b**) relative mass loss, and (**d**) mass% chromium concentration
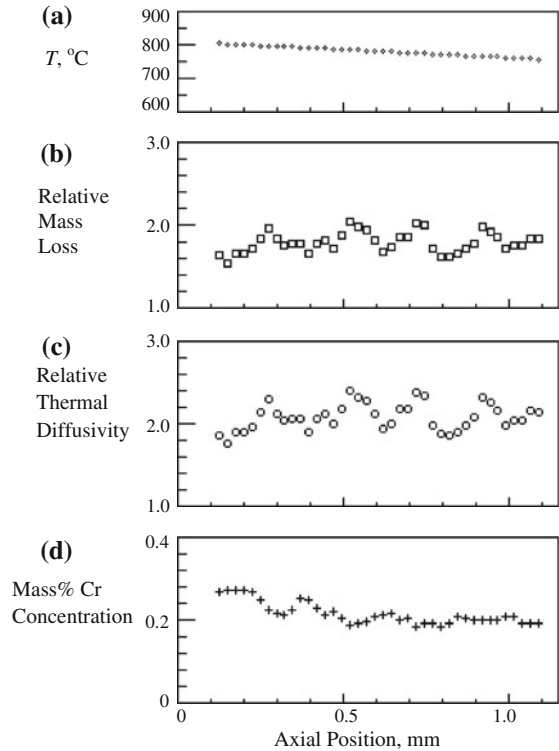
layer. The composition has been measured in this study for each LPP excitation, as stated above, and we thus find the molar mass as a function of temperature;

$$M(T) = [1 - C_{Cr}(T)]M_{Ni} + C_{Cr}(T)M_{Cr}, \qquad (6)$$

where M_{Ni} and M_{Cr} are the molar masses of nickel and chromium, respectively. $C_{Cr}(T)$ denotes the concentration of chromium at temperature T.

The mass loss measurement is converted into the relative thermal diffusivity of the Nichrome specimen according to Eq. 3, and the results are shown in Fig. 2c as a function of position within the laser focal area, together with the local temperature (Fig. 2a), relative mass loss (Fig. 2b), and elemental composition (Fig. 2d). The temperature of the specimen at the center of the laser focal spot is 1,033 K. The results show that LPP plume spectroscopy is successful in detecting the temperature gradient imposed on the specimen both in terms of position-dependent changes in elemental composition and in the detected relative mass loss as a function of position along an axis parallel to the long axis of the specimen ribbon. It is interesting to note that the chromium concentration versus position dependence is not monotonic at all temperatures. In fact, Fig. 3b shows a shallow minimum in the middle of the laser focal spot when the specimen temperature is centered at 869 K.
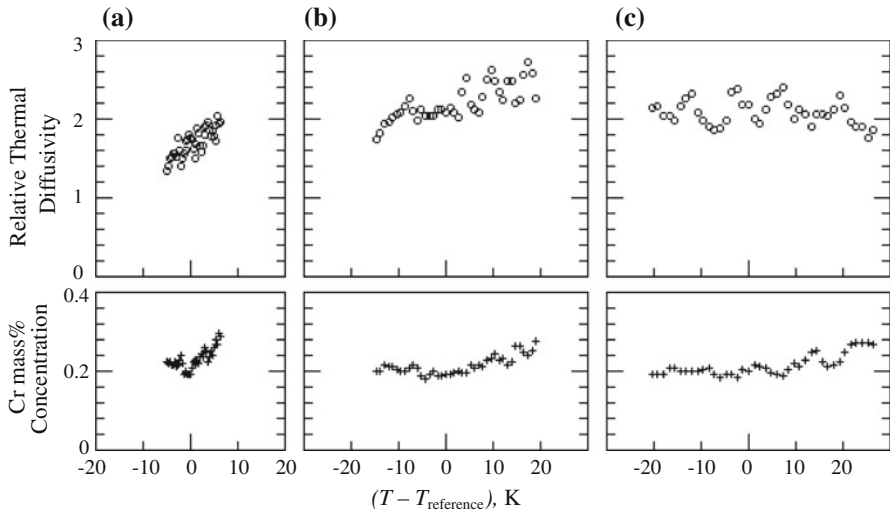
Fig. 3 Relative thermal diffusivity (*circles*) and mass% chromium concentration (*crosses*) of a Nichrome specimen at three elevated temperatures, relative to a fresh Nichrome specimen at room temperature as a reference, are shown. The specimen was heated nonuniformly, and measurements of both thermal diffusivity and chromium concentration were made simultaneously at multiple temperatures. The results are shown for each group as a function of specimen temperature relative to a reference temperature $T_{reference}$: (**a**) $T_{reference} = 869$ K, (**b**) $T_{reference} = 1,033$ K, and (**c**) $T_{reference} = 1,150$ K

The specimen was examined at two other temperatures, 869 K and 1,150 K. The three sets of relative thermal diffusivity data are combined and shown as a function of temperature in Fig. 3; also shown in the figure are the three corresponding groups of values of the chromium concentration as a function of temperature. The three groups of relative thermal diffusivity values appear reasonably consistent with each other. The relative thermal diffusivity values are consistently trended in their temperature dependence with other literature values for alloys that are nickel-based, that is, the thermal diffusivity is significantly higher in the elevated temperature range than it is at room temperature [12,13].

On the other hand, the relative thermal diffusivity values within a group (see Fig. 2) indicate a sensitive temperature dependence that is different from the groups at other temperatures. The chromium concentration profile shows a significant dependence on the temperature range at which each group is centered. It is reasonable to suggest that the structure of the relative thermal diffusivity as a function of temperature is highly variable, interspersed with large amplitude variations. The key factor seems to be the local elemental composition, and the composition varies depending sensitively on the temperature and the length of thermal forcing. In each of the groups of measurements shown here, the length of thermal forcing has been limited to less than 20 min.

We note that the thrust of this investigation is to examine how the thermal diffusivity of an alloy (Nichrome) changes as a function of temperature. For this reason, we have used the thermophysical properties of a fresh specimen of the alloy at room temperature as a reference, and the results are presented in the form of relative thermal diffusivity.

5 Conclusions

The measurement of thermophysical properties for multielement alloys encounters numerous issues that are associated with the fact that constituent elements undergo diffusion at elevated temperatures. The process results in an elemental-composition profile that is position dependent within the specimen. The profile evolves as a function of temperature and the length of thermal forcing, and is thus cumulative. In an attempt to identify an effective new criterion for such measurements for alloys, we have examined the full range of issues in carrying out simultaneous multitemperature measurement by means of the method of time-resolved spectroscopy of LPP plume emissions. When a Nichrome specimen is heated nonuniformly, it is indeed possible to measure the thermal diffusivity and elemental composition as a function of temperature all within the footprint of a single laser pulse. The thermal-diffusivity values are consistent in temperature dependence with literature values for other nickel-based alloys, although comparisons under identical specimen conditions are not possible at this time.

The measurement uncertainty has a number of contributing sources. The largest source is in photon counting for the mass loss and composition detection because a single two-dimensional (2D) array detector is now divided into 256 detection channels so that 256 positions on the specimen surface can be analyzed. Typically, several hundred photoelectrons are registered on average, raising the counting uncertainty to 6.0%; off the center of the laser focal spot, this can rise to 8%. Others include the uncertainties in measurements of the temperature, the temperature gradient, and the mismatch between the temperature versus position calibration and the mass loss versus position measurement; they may add up to 1% in temperature assignment. A slow creeping upward of the specimen temperature during the 17 min period needed to prepare the specimen for three different temperatures can cause a change in the elemental composition profile. This would affect the intrinsic mass loss measure due to composition uncertainty; we estimate this to be 5%. The overall uncertainty in the relative thermal diffusivity may be as large as 10% to 15% at present.

A direct method of establishing the uncertainty would be to carry out a suite of measurements with a large number of specimens. At the same time, the uncertainty may be reduced by a set of adjustments to the measurement procedure: (a) the 1:1 magnification of the specimen's image at the plane of the entrance slit of the spectrograph may be reduced to increase the photoelectron counts at the detector; (b) use of three thermocouple junctions so that the temperature and its gradient can be measured simultaneously, preferably welded to the back of the specimen [14]; and (c) increase of the ambient gas pressure in the vacuum chamber will slightly impede the expansion of the LPP plume and thus increase LPP plume emission intensities. Reduction of the uncertainty to 3% to 5% is within the realm of possibility.

Development of a comprehensive understanding of thermophysical properties of disordered metallic alloys is highly desirable because the number of alloys is very large and their functionality wide ranged. Their applications not only cover the full spectrum of materials usage but also impact the efficiency of energy production and utilization. Significant improvement in materials utilization will hinge on developing a cause-and-effect relationship of a material specimen's elemental composition structure and transport of excitations through the material medium.

References

1. Y.W. Kim, Int. J. Thermophys. **23**, 1103 (2002)
2. Y.W. Kim, Int. J. Thermophys. **28**, 732 (2007)
3. Y.W. Kim, High Temp.-High Press. **38**, 1 (2009)
4. Y.W. Kim, *Thermal Conductivity 26*, ed. by R.B. Dinwiddie (DEStec Pubs, Lancaster, PA, 2005), pp. 146–158
5. Y.W. Kim, Int. J. Thermophys. **14**, 397 (1993)
6. Y.W. Kim, Int. J. Thermophys. **28**, 1037 (2007)
7. Y.W. Kim, in *Laser-Induced Plasmas and Applications*, ed. by L.J. Radziemski, D.A. Cremers (Marcell Dekker, New York, 1989)
8. Y.W. Kim, N. Poolyarat, Rev. Sci. Instrum. **79**, 10E715 (2008)
9. G. Narsimhan, J. Phys. Chem. **67**, 2238 (1963)
10. Y.Z. Zhang, Int. J. Thermophys. **10**, 911 (1989)
11. C. Cheng, X. Xu, Int. J. Thermophys. **28**, 9 (2007)
12. Y.S. Touloukian, R.W. Powell, C.Y. Ho, M.C. Nicolaou, *Thermal Diffusivity* (Plenum, New York, 1973)
13. A. Hazotte, B. Perrot, P. Archambaut, J. Phys. IV **3**, 351 (1993)
14. K. Maglić, A. Dobrosavljević, N. Perović, A. Stanimirović, G. Vuković, *High Temp. High Press.* **27/28**, 389 (1995/1996)